PCCP

COMMUNICATION

View Article Online
View Journal | View Issue

Cite this: *Phys. Chem. Chem. Phys.*, 2015, **17**, 27275

Received 27th July 2015,
Accepted 13th September 2015

DOI: 10.1039/c5cp04401d

www.rsc.org/pccp

Picosecond melting of peptide nanotubes using an infrared laser: a nonequilibrium simulation study†

Man Hoang Viet,[a] Phan Minh Truong,[b] Philippe Derreumaux,[cd] Mai Suan Li,*[be] Christopher Roland,*[a] Celeste Sagui*[a] and Phuong H. Nguyen*[f]

Self-assembled functional peptide biomaterials are emerging with a wide range of envisioned applications in the field of nanotechnology. Currently, methods and tools have been developed to control and manipulate as well as to explore new properties of self-assembled structures. However, considerably fewer studies are being devoted to developing efficient methods to degrade or recycle such extremely stable biomaterials. With this in mind, here we suggest a theoretical framework, inspired by the recent developed mid-infrared free-electron laser pulse technology, to dissociate peptide nanotubes. Adopting a diphenylalanine channel as a prototypical example, we find that the primary step in the dissociation process occurs due to the strong resonance between the carboxylate bond vibrations of the diphenylalanine peptides and the tuned laser frequencies. The effects of laser irradiation are determined by a balance between tube formation and dissociation. Our work shows a proof of concept and should provide a motivation for future experimental developments with the final aim to open a new and efficient way to cleave or to recycle bio-inspired materials.

Introduction

A number of proteins and peptides have been found to aggregate into insoluble amyloid fibrils. In their basic structure, fibrils are predominantly composed of cross-β-sheets and stabilized by a hydrogen bond (HB) network.[1,2] Such natural biopolymer aggregates often exhibit unusual material properties, such as a pull strength comparable to that of steel, mechanical shear stiffness similar to that of silk, as well as extreme persistence length and mechanical rigidity.[3,4] Therefore, amyloid fibrils have been recently exploited for the generation of novel biological materials.[5]

An extensively studied short, self-assembling peptide is diphenylalanine NH_3^+–Phe–Phe–COO^- (FF), a fragment of the Alzheimer's β-amyloid peptide. Görbitz first showed that this dipeptide can form channel structures through X-ray crystallographic analysis.[6] Later, it has been shown that FF can also self-assemble into highly ordered nanotubes/microtubes,[5,7,8] micro-crystals,[9] vertically aligned nanowires[10] and nanoforests,[11] depending on the concentration. Among these structures, the FF nanotubes are of special interest due to their unique physical, chemical and mechanical properties. For example, the FF nanotubes possess a high Young's modulus of ≈19 GPa, a strong stiffness of 160 N m^{-1},[12] and are stable under extreme conditions, including boiling water, organic solvents such as ethanol, acetone and various acidic conditions.[13,14] The robust nature of FF nanotubes makes them extremely practical in many applications. For example, FF nanotubes have been deposited on the surface of screen-printed graphite and gold electrodes to improve their sensitivity for biosensing.[15] The internal hole of the FF nanotubes was used as a template for forming silver nanowires.[5] For excellent reviews of the properties and applications of FF nanotubes, readers are referred to recent publications.[16–23] While most of current research focuses on the fabrication and applications of FF nanotubes, fewer studies have been carried out to address an obvious concern: how to efficiently dissociate such extremely robust materials without causing much damage to the surrounding environment? This concern should be important if one wants to translate the peptide-based nanofabrication technology into real-world applications where the degradation and recycling of materials might be necessary. Just one intuitive example is how to remove the template without causing much damage to the silver nanowires in the experiment using the FF nanotube as a template to grow silver nanowires?[5] Obviously, the use of acidic conditions or high temperatures[14] is not promising because the surrounding medium is easily affected.

Recently, a new laser technology has been developed and applied to the amyloid-based materials.[24–30] In particular, Kawasaki

[a] *Department of Physics, North Carolina State University, Raleigh, NC 27695-8202, USA. E-mail: cmroland@ncsu.edu, sagui@ncsu.edu*
[b] *Institute for Computational Science and Technology, Quang Trung Software City, Tan Chanh Hiep Ward, District 12, Ho Chi Minh City, Vietnam*
[c] *Laboratoire de Biochimie Theorique, UPR 9080 CNRS, IBPC, Universite Denis Diderot, Paris Sorbonne Cité 13 rue Pierre et Marie Curie, 75005, Paris, France*
[d] *Institut Universitaire de France, Bvd Saint Michel, 75005, Paris, France*
[e] *Institute of Physics, Polish Academy of Sciences, Al. Lotnikow 32/46, 02-668 Warsaw, Poland. E-mail: masli@ifpan.edu.pl*
[f] *Laboratoire de Biochimie Theorique, UPR 9080 CNRS, IBPC, Universite Paris 7, 13 rue Pierre et Marie Curie, 75005, Paris, France. E-mail: nguyen@ibpc.fr*

† Electronic supplementary information (ESI) available Details of the construction and characterization of the FFC, equilibrium and NEMD simulations. See DOI: 10.1039/c5cp04401d

and coworkers have developed a mid-infrared free-electron laser (FEL) having specific oscillation characteristics of a picosecond pulse structure, a tunable wavelength within infrared frequencies and a high photon density. Tuning the laser frequency to that of the amide I bands, they were able to dissociate amyloid-like fibrils of lysozyme into their native forms,[27] convert insulin fibrils into soluble monomers[28] and dissociate a fibril of a short peptide from the human thyroid hormone.[29,30] Inspired by this type of experiments, here we show, as a proof of concept, that the FF nanotubes can be degraded by FEL whose frequency is tuned to the vibrational frequency of the carboxylate groups of the FF peptides. With this in mind, we first construct a model FF channel, then characterize the equilibrium structure by carrying out a long all-atom molecular dynamics (MD) simulation in explicit water, and finally, subject the equilibrium structures to nonequilibrium MD (NEMD) simulations where laser pulses are applied within 500 ps resulting in the dissociation of the tube.

Construction of the FF channel

X-ray crystallographic analysis[6] has shown that the wall of a FF nanotube is formed by many small FF channels (FFCs), and each individual FFC is circled by merely six FF peptides. In such an arrangement, the termini NH_3^+ and COO^- of each peptide point toward the center of the tube, and the two phenyl groups pointing outward to the two phenyl groups of another FF of neighboring channels [Fig. 1(A)]. Thus, the wall thickness of an FFC consists of only two FFs. As a proof of concept, we limit ourselves to consider only a single FFC in this work. To this end, we take a single FF peptide, which is in the *cis*-state, from the crystal structure (CCDC 163340) and employ the 2D lattice wrapping system method recently developed by Nussinov and coworkers[31,32] to construct a FFC model. Our FFC consists of twelve complete double-circles, each consisting of twelve FF peptides [Fig. 1(B) and (C)] resulting in 144 FFs in total. The diameter and length of the FFC after energy minimization *in vacuo* using the Gromos43a1 force field[33] are $\langle D \rangle$ = 2.56 nm and $\langle L \rangle$ = 6.51 nm, respectively. The HB network that stabilizes the FFC is formed between the termini ($-NH_3^+ \cdots {}^-COO-$) of consecutive peptides in each circle (intra-circle HB), of adjacent peptides between neighboring circles (inter-circle HB) and between the amide N and carboxylate hydrogen motifs ($-NH- \cdots {}^-COO-$). The hydrophobic and π-stacking interactions between side chains of FF peptides also contribute to the stability of the channel. Details of the construction and characterization of the FFC can be found in the ESI.†

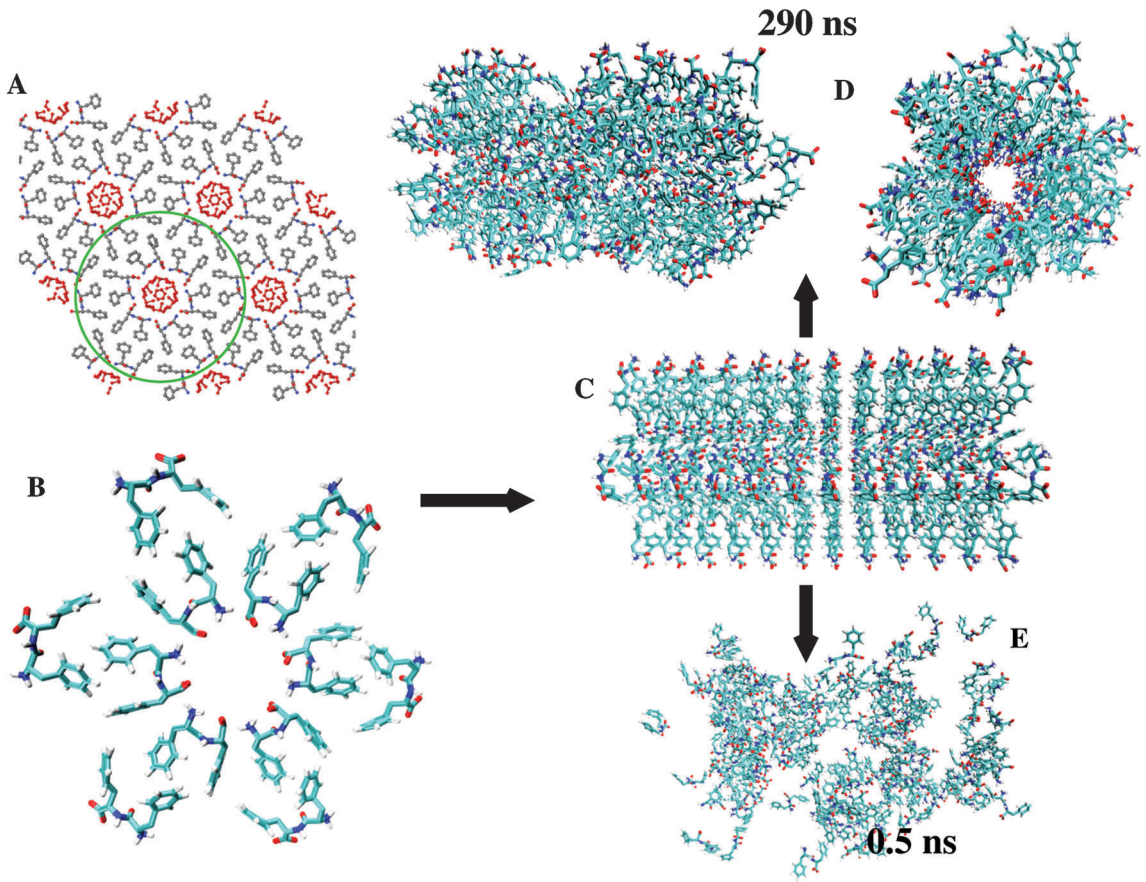

Fig. 1 (A) Cross section of the crystal structure of FF nanotubes. The green circle indicates a FF channel (FFC) in which water molecules (red points) are localized at the centre of the channel. (B) One complete circle of the constructed FFC consisting of an inner and an outer circle, each containing six FF peptides. (C) The FFC constructed in 12 circles. (D) A selected equilibrium structure (left: side view, right: top view) after 290 ns of the conventional MD simulation. (E) A selected structure after 0.5 ns of the NEMD laser-induced dissociation.

Equilibrium structure

Next, we wish to obtain the equilibrium structure of the constructed FFC. To this end, we solvate it inside a cubic box with 20650 SPC waters[34] (concentration of 300 mM) and carry out a 290 ns MD simulation at a temperature of 315 K, using the Gromos43a1 force field[33] and the GROMACS simulation package. The details of the simulation can be found in the ESI.†

During the time evolution the FFC relaxes to less ordered conformations, as indicated by fluctuations in the radius of gyration, length and diameter [Fig. 2(A)–(C)], but the overall tubular structure is maintained [Fig. 1(D)]. The FFC is still primarily stabilized by the intra- and inter-circles (–$NH_3^+\cdots{}^-$COO–) HBs, which do not show any significant changes [Fig. 2D]. A closer inspection reveals that the inner channel is much more stable as it is protected from the waters by the outer channel. To understand the detailed interactions that stabilize the FFC, we calculate the Coulomb and van der Waals (vdW) interaction energies between side-chains and between termini. As seen from Fig. 2(E) and (F) the vdW interaction between side-chains, and Coulomb interaction between termini contribute significantly to the stability of the intra- and inter-circle structures. This is consistent with previous coarse-grained and all-atom simulations which showed that the FF nanotubes are stabilized by a combination of both aromatic stacking and inter-peptide head-to-tail hydrogen-bonding.[35–37] From this equilibrium trajectory, we select 100 independent structures for subsequent NEMD simulations.

Laser-induced nonequilibrium simulation

Next we wish to show that the stable equilibrium FFC can be degraded under infrared picosecond laser irradiation. To this end, we carried out NEMD simulations starting from 100 structures selected above. In the NEMD simulation, a time-dependent electric field

$$E(t) = E_0 \exp\left[-\frac{(t-t_0)^2}{2\sigma^2}\right]\cos[2\pi c\omega(t-t_0)], \qquad (1)$$

was applied to mimic a laser micro-pulse. Here, E_0 represents the amplitude of the electric field, σ is the pulse width, t is the time after the pulse maximum t_0, c is the speed of light and ω is the frequency. In a conventional MD simulation, the temperature of the system is typically maintained by rescaling the velocities of all atoms at every time step.[38] In a laser-induced nonequilibrium experiment, the photo-excitation results in a vibrationally hot molecule, which is then cooled *via* transfer of the vibrational energy to the surrounding solvent molecules.[39] Thus, in our NEMD simulations, only the waters are coupled to the heat bath in order to maintain the temperature of 310 K with a coupling constant of 0.1 ps. This technique has been developed in previous photo-induced NEMD simulations of peptides[39–44] and validated by comparing the cooling times with known experimental results.[39,42] This also mimics the experimental conditions, in which water is added periodically to the suspension during the irradiation process[29] in order to prevent excessive evaporation. To ensure stability, a time step of 0.2 fs was used, and data were collected every 0.1 ps.

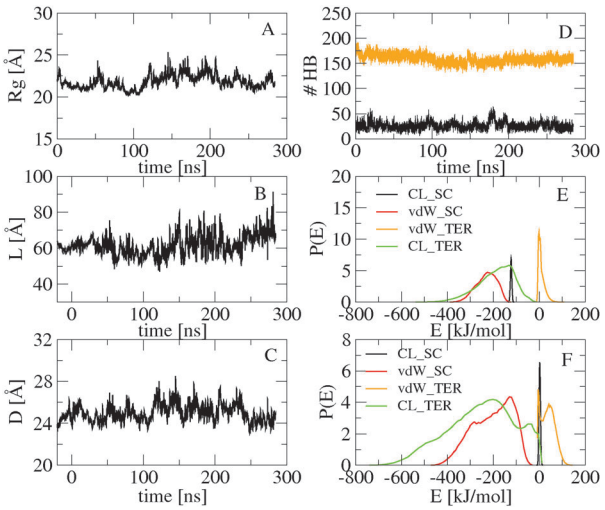

Fig. 2 Time evolution of the FFC radius of gyration (A), length (B) and diameter (C). In (D) the time evolution of the (–$NH_3^+\cdots{}^-$COO–) intra-(black) and inter-circle (orange) HBs. In (E) the distribution of the intra-circle interaction energies. Shown are results of the Coulomb energy between side-chains (black), termini (green), and van der Waals energy between side-chains (red), termini (orange). (F) is the same as (E) but for inter-circle energies.

Resonance between carboxylate bond vibrations and laser field

In FEL experimental studies, a macro-pulse consists of a train of micro-pulses of 2 ps duration separated by a time interval of 350 ps, and the energy of the laser pulse is in the range of 6–8 mJ.[27–30] To mimic this experimental condition, we set the pulse width of our laser at σ = 2 ps, t_0 = 10 ps and the strength E_0 = 5 V nm^{-1} so that the FFC dissociates within a reasonable timescale. To obtain the optimal frequency, we carry out 20 sets of NEMD simulations (each lasting 50 ps) using single laser pulse with ω varying from 1620 to 1680 cm^{-1} with a step of 2 cm^{-1}. The electric field, [eqn (1)], is shown in Fig. 3(A). To illustrate the system response to the field, we show in Fig. 3 the system total energy, the fluctuations of the C=O amide I and the carboxylate COO^- bonds, the total number of inter-circle (–$NH_3^+\cdots{}^-$COO–) HBs and the tube radius of gyration. As seen, the FFC exhibits a strong resonance with the field at ω = 1648 cm^{-1}, which represents the peak of the carboxylate bond vibrations of the FFC [Fig. 3(B) and Fig. S2, ESI†], as indicated by large changes in the total energy and the COO^- bond lengths [Fig. 3(C) and (D)]. The FFC tends to be degraded as shown by the decrease of the HB number from the equilibrium value of 180 to 110 HBs, and the radius of gyration increase from 23 Å to 55 Å [Fig. 3(E) and (F)]. Given the fact that the (–$NH_3^+\cdots{}^-$COO–) HBs are the main contributions to the FFC stabilization, the resonance of the COO^- bond vibrations and the dissociation of the FFC at the same frequency indicate that the laser excites primarily the COO^- bonds of the FFC, and that these

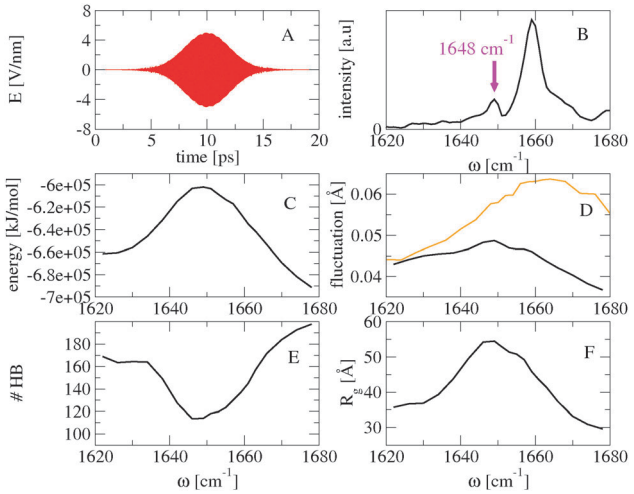

Fig. 3 (A) Time evolution of the electric field with ω = 1648 cm^{-1}, E_0 = 5 V nm^{-1}; (B) vibrational IR spectrum of the FFC equilibrium structure; (C) laser-induced changes of the system energy; (D) fluctuations of C=O amide I (orange) and COO^- (black) bond lengths; (E) the number of inter-circle HBs and (F) radius of gyration. Results are shown for the laser amplitude E_0 = 5 V nm^{-1} and different frequencies ω.

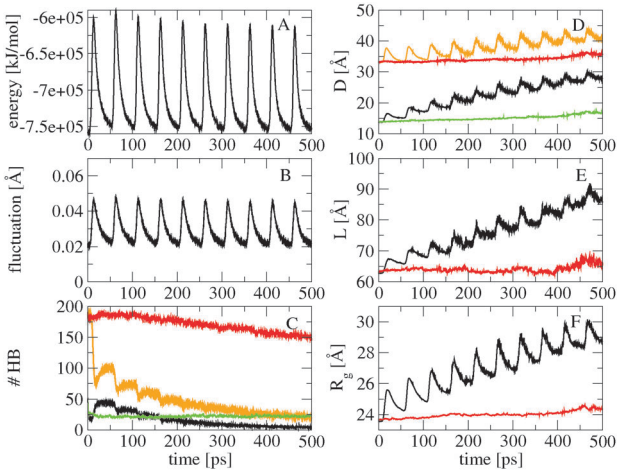

Fig. 4 (A) Time evolution of the energy of the system; (B) fluctuation of the carboxylate COO^- bonds; (C) the number of the intra- (black, green) and inter-circle (orange, red) Hbs; (D) the diameters of the inner (black, green) and outer (orange, red) channel; (E) the length; (F) the radius of gyration of the FFC. Shown are the results obtained from the NEMD simulation using 10 micro-pulses with ω = 1648 cm^{-1}, E_0 = 5 V nm^{-1} (black, orange), and the equilibrium simulation at T = 500 K (green, red).

are enough to dissociate the FFC. The C=O amide bonds are also in resonance with the field but at a higher frequency ω = 1660 cm^{-1} [Fig. 3(B) and (D)]. They do not contribute much to the dissociation process because these bonds are less involved in the HB network that stabilizes the FFC.[6] In the following, we use the laser frequency of ω = 1648 cm^{-1} to investigate the dissociation mechanism.

Laser-induced FFC dissociation process

Under irradiation of a single micro-pulse the FFC is destabilized but the tubular structure is largely maintained, thus we use multiple pulses as done in experiments of fibril dissociation.[27–30] To this end, starting from 100 selected equilibrium MD conformations, we carry out NEMD simulations, each lasting 500 ps. During this time, 10 micro-pulses of σ = 2 ps duration separated by a time interval of 20 ps are applied to the system. We should note that this time interval is quite short, and difficult to generate in real experiments. Nevertheless, given the large system-size of the FFC and as our main aim is to provide a proof of concept, this toy laser model allows us to dissociate the FFC within reasonable simulation timescale without loss of the general conclusions. As seen from Fig. 4(A), under the irradiation of the first pulse the system absorbs energy after 2 ps and the energy increases from the equilibrium value to its maximal value at around 10 ps, which represents the peak of the laser pulse [Fig. 3(A)]. After 15 ps the pulse vanishes, the system cools down and the system energy reaches its equilibrium value at around 50 ps. During the excitation the carboxylate COO^- bonds are excited and their bond lengths fluctuate at around the equilibrium value of 1.25 Å with the maximal amplitude of $\approx$0.05 Å [Fig. 4(B)]. As a consequence, intra- and inter-circle HBs formed in the equilibrium structures are excited, broken and reduced from the initial values of $\approx$50 to $\approx$19 HBs for the former, and from 180 to $\approx$95 HBs for the latter within the first 15 ps [Fig. 4(C)]. This leads to the destabilization of the FFC as indicated by the increases of the diameters, length and radius of gyration [Fig. 4(D–F)]. However, as shown in Fig. 2(E) and (F), the van der Waals interaction between side-chains also contributes significantly to the stabilization of the FFC; therefore, at $t \geq$ 15 ps (laser is turned off), this interaction forces the system to quickly refold back to initial structure, as indicated by the increases of the HBs as well as of the other structural quantities. This suggests that there is a delicate balance between the tube formation and dissociation. Understanding the factors that are responsible for this balance might provide important insights into the self-assembly mechanisms. After 50 ps, the laser is turned on again and the second pulse excites the system one more time leading to further destabilization. Although there is always a competition between the reformation and dissociation processes, the latter eventually wins resulting in complete dissociation after 500 ps [Fig. 1(E)]. Note that because more termini ($NH_3^+\cdots{}^-COO$–) HBs are formed in the inner channel than in the outer one [Fig. 1(B)], the inner channel absorbs more energy. This results in a large change in its diameter, from 10 to 25 Å, while that of the outer channel increases only from 35 to 40 Å [Fig. 4(D)].

Finally, to compare the laser-induced dissociation with that induced by thermal effects we carried out an equilibrium simulation at 500 K. At this temperature, in the classical approximation each vibrational mode carries an energy of $k_BT \approx$ 1 kcal mol^{-1}. As seen from Fig. 4, the conformational changes take place slowly as reflected by the overall slow decay in the number of HBs [Fig. 4(C)] as well as in the other structural quantities [Fig. 4(D)–(F)]. We should note that the reductions in the intra- and inter-circle HBs are also observed at $t \leq$ 2 ps, which is simply due to the relaxation of the initial constructed structure. In contrast, the laser deposits

energy directly into the COO^- bonds, and so the dissociation takes place much faster, since it is these HBs that hold the structure together. This confirms that the laser-induced FFC dissociation process observed in our NEMD simulation is localized, and is not due to just thermal effects.

Concluding remarks

We have presented comprehensive laser-induced NEMD simulations, and have shown that by tuning the laser frequency precisely to that of the carboxylate COO^- bond stretching vibrational modes, one is able to degrade a model FF channel. The simulation shows that the dissociation is initiated by the laser-excitation of these particular modes, and not by the infrared thermal effects. This allows one to degrade peptide nanotubes precisely, without much heating and damage to the surrounding environment. We find that during the dissociation process there is always a balance between the tube formation and dissociation. This reflects the high resistance properties of peptide nanotubes. Understanding the factors that are responsible for this balance may be important in the design of peptide-based materials. Although the proposed method is demonstrated for only one FF channel, it should also be applicable for a class of self-assembled peptide structures with the same dissociation mechanism. This is because most of these structures share the same stability characteristics, which is attributed to the highly cooperative nature of the HB network throughout the lattice.[45] The C═O or COO^- bonds, which participate in that HB network, can be excited due to strong resonance with the laser field, leading to the destabilization of the HB network and subsequently dissociation of the whole structures. Given the success of Kawasaki and coworkers in the development and application of the mid-infrared FEL for the dissociation of amyloid fibrils,[27–30] we believe that this class of experiments should also be feasible for the dissociation of self-assembled peptide nanomaterials. The laser-induced dissociation method may thus open up new opportunities for the efficient cleavage and recycling of peptide-based nanomaterials.

Acknowledgements

This work has been supported by the Department of Science and Technology at Ho Chi Minh City, Vietnam (grant 186/HD-SKHCN), the CNRS, IUF and the National Science Foundation USA (NSF) *via* grant SI2-1148144. We are grateful to IDRIS for providing computer facilities (grant x2015077198).

References

1 F. Chiti and C. M. Dobson, Protein misfolding, functional amyloid and human disase, *Annu. Rev. Biochem.*, 2006, **75**, 333–366.
2 J. Nasica-Labouze, P. H. Nguyen, F. Sterpone, O. Berthoumieu, N. V. Buchete, S. Cote, A. De Simone, A. J. Doig, P. Faller, A. Garcia, A. Laio, M. S. Li, S. Melchionna, N. Mousseau, Y. Mu, A. Paravastu, S. Pasquali, D. J. Rosenman, B. Strodel, B. Tarus, J. H. Viles, T. Zhang, C. Wang and P. Derreumaux, Amyloid β protein and Alzheimer's disease: when computer simulations complement experimental studies, *Chem. Rev.*, 2015, **115**, 3518–3563.
3 J. Smith, T. P. Knowles, C. M. Dobson, C. MacPhee and M. Welland, Characterization of the nanoscale properties of individual amyloid fibrils, *Proc. Natl. Acad. Sci. U. S. A.*, 2006, **103**, 15806–15811.
4 A. W. Fitzpatrick, G. Vanacore and A. Zewail, Nanomechanics and intermolecular forces of amyloid revealed by four-dimensional electron microscopy, *Proc. Natl. Acad. Sci. U. S. A.*, 2015, **112**, 3380–3385.
5 M. Reches and E. Gazit, Casting metal nanowires within discrete self-assembled peptide nanotubes, *Science*, 2003, **300**, 625–627.
6 C. H. Gorbitz, Nanotube formation by hydrophobic dipeptides, *Chem. – Eur. J.*, 2001, **7**, 5153.
7 L. Adler-Abramovich, D. Aronov, P. Beker, M. Yevnin, S. Stempler, L. Buzhansky, G. Rosenman and E. Gazit, Self-assembled arrays of peptide nanotubes by vapour deposition, *Nat. Nanotechnol.*, 2009, **4**, 849–854.
8 M. Wang, L. Du, X. Wu, S. Xiong and P. K. Chu, Charged diphenylalanine nanotubes and controlled hierarchical self-assembly, *ACS Nano*, 2011, **5**, 4448–4454.
9 P. Zhu, X. Yan, Y. Yang and J. Li, Solvent-induced structural transition of self-assembled dipeptide: from organogels to microcrystals, *J. Chem.*, 2010, **16**, 3176–3183.
10 J. Ryu and C. B. Park, High-temperature self-assembly of peptides into vertically well-aligned nanowires by aniline vapor, *Adv. Mater.*, 2008, **20**, 3754–3758.
11 M. Reches and E. Gazit, Controlled patterning of aligned self-assembled peptide nanotubes, *Nat. Nanotechnol.*, 2006, **1**, 195–200.
12 N. Kol, L. Adler-Abramovich, D. Barlam, R. Z. Shneck, E. Gazit and I. Rousso, Self-assembled peptide nanotubes exhibit unique mechanica stiffness, *Nano Lett.*, 2005, **5**, 1343–1346.
13 L. Adler-Abramovich, M. Reches, V. L. Sedman, S. Allen, S. J. B. Tendler and E. Gazit, Thermal and chemical stability of diphenylalanine peptide nanotubes: Implications for nanotechnological applications, *Langmuir*, 2006, **22**, 1313.
14 J. Ryu and C. H. Park, High stability of self-assembled peptide nanowires against thermal, chemical and proteolytic attacks, *Biotechnol. Bioeng.*, 2010, **105**, 221–230.
15 M. Yemini, M. Reches, J. Rishpon and E. Gazit, Novel electrochemical biosensing platform using self-assembled peptide nanotubes, *Nano Lett.*, 2005, **5**, 183–186.
16 X. Zhao, F. Pan and J. R. Lu, Recent development of peptide self-assembly, *Prog. Nat. Sci.*, 2008, **18**, 653–660.
17 S. Scanlon and A. Aggeli, Self-assembling peptide nanotubes, *Nano Today*, 2008, **3**, 22–30.
18 X. Yan, P. Zhu and J. Li, Self-assembly and application of diphenylalanine-based nanostructures, *Chem. Soc. Rev.*, 2010, **39**, 1877–1890.
19 C. Valery, F. Artzner and M. Paternostre, Peptide nanotubes: molecular organisations, self-assembly mechanisms and applications, *Soft Matter*, 2011, **7**, 9583–9594.
20 A. Lakshmanan, S. Zhang and C. A. E. Hauser, Short self-assembling peptides as building blocks for modern nanodevices, *Trends Biotechnol.*, 2011, **30**, 155–165.

21 A. B. Seabra and N. Duran, Biological applications of peptides nanotubes: An overview, *Peptides*, 2013, **39**, 47–54.
22 I. W. Hamley, Peptide nanotubes, *Angew. Chem., Int. Ed.*, 2014, **53**, 2–18.
23 L. Adler-Abramovich and E. Gazit, The physical properties of supramolecular peptide assemblies: from building block association to technological applications, *Chem. Soc. Rev.*, 2014, **43**, 6881–6893.
24 P. Hanczyc, M. Samoc and B. Norden, Multiphoton absorption in amyloid protein fibers, *Nat. Photonics*, 2013, **7**, 969–972.
25 D. Ozawa, H. Yagi, T. Ban, A. Kameda, T. Kawakami, H. Naiki and Y. Goto, Destruction of amyloid fibrils of a β-microglobulin fragment by laser beam irradiation, *J. Biol. Chem.*, 2009, **284**, 1009–1017.
26 H. Yagi, D. Ozawa, K. Sakurai, T. Kawakami, H. Kuyama, O. Nishimura, T. Shimanouchi, R. Kuboi, H. Naiki and Y. Goto, Laser-induced propagation and destruction of amyloid β fibrils, *J. Biol. Chem.*, 2010, **285**, 19660–19667.
27 T. Kawasaki, J. Fujioka, T. Imai and K. Tsukiyama, Effect of mid-infrared free-electron laser irradiation on refolding of amyloid-like fibrils of lysozyme into native form, *Protein J.*, 2012, **31**, 710–716.
28 T. Kawasaki, J. Fujioka, T. Imai, K. Torigoe and K. Tsukiyama, Mid-infrared free-electron laser tuned to the amide i band for converting insoluble amyloid-like protein fibrils into the soluble monomeric form, *Lasers in Medical Science*, 2014, **29**, 1701–1707.
29 T. Kawasaki, T. Imai and K. Tsukiyama, Use of a mid-infrared free-electron laser (mir-fel) for dissociation of the amyloid fibril aggregates of a peptide, *J. Anal. Sci., Methods Instrum.*, 2014, **4**, 9–18.
30 T. Kawasaki, T. Yaji, T. Imai, T. Ohta and K. Tsukiyama, Synchrotron-infrared microscopy analysis of amyloid fibrils irradiated by mid-infrared free- electron laser, *Am. J. Anal. Chem.*, 2014, **5**, 384–394.
31 C. J. Tsai, J. Zheng and R. Nussinov, Designing if nanotube using naturally occurring protein building blocks, *PLoS Comput. Biol.*, 2006, **2**, e24.
32 C. J. Tsai, J. Zheng, D. Zanuy, N. Haspel, H. Wolfson, C. Aleman and R. Nussinov, Principles of nanostructure design with protein buidling blocks, *Protein J.*, 2007, **68**, 1–12.
33 W. van Gunsteren, S. R. Billeter, A. A. Eising, P. H. Hünenberger, P. Krüger, A. E. Mark, W. Scott and I. Tironi, *Biomolecular Simulation: The GROMOS96 Manual and User Guide.*, Vdf Hochschulverlag AG an der ETH, Zurich, 1996.
34 H. J. C. Berendsen, J. Postma, W. van Gunsteren and J. Hermans, *Intermolecular Forces*, Reidel, Dortrecht, 1996.
35 P. Tamamis, L. Adler-Abramovich, M. Reches, K. Marshall, P. Sikorski, L. Serpell, E. Gazit and G. Archontis, Self-assembly of phenylalanine oligopeptides: Insights from experiments and simulations, *Biophys. J.*, 2009, **96**, 5020–5029.
36 J. Jeon, C. E. Mills and M. S. Shell, Molecular insights into diphenylalanine nanotube assembly: all atom simulations of oligomerization, *J. Phys. Chem. B*, 2013, **117**, 3935–3943.
37 C. Guo, Y. Luo, R. Zhou and G. Wei, Probing the self-assembly mechanism of diphenylalanine based peptide nanovesicles and nanotubes, *ACS Nano*, 2010, **5**, 3907–3918.
38 H. J. C. Berendsen, J. P. M. Postma, W. F. van Gunsteren, A. Dinola and J. R. Haak, Molecular-dynamics with coupling to an external bath, *J. Chem. Phys.*, 1984, **81**, 3684–3690.
39 V. V. Botan, E. H. G. Backus, R. Pfister, A. Moretto, M. Crisma, C. Toniolo, P. H. Nguyen, G. Stock and P. Hamm, Energy transport in peptide helices, *Proc. Natl. Acad. Sci. U. S. A.*, 2007, **104**, 12749.
40 P. Nguyen and G. Stock, Nonequilibrium molecular dynamics simulation of a photoswitchable peptide, *Chem. Phys.*, 2006, **323**, 36.
41 P. Nguyen, R. D. Gorbunov and G. Stock, Photoinduced conformational dynamics of a photoswitchable peptide: A nonequilibrium molecular dynamics simulation study, *Biophys. J.*, 2006, **91**, 1224.
42 E. H. G. Backus, P. H. Nguyen, V. Botan, R. Pfister, A. Moretto, M. Crisma, C. Toniolo, G. Stock and P. Hamm, Energy transport in peptide helices: A comparison between high- and low-energy excitations, *J. Phys. Chem. B*, 2008, **112**, 9091.
43 S. Y. Park, P. H. Nguyen and G. Stock, Molecular dynamics simulation of cooling: Heat transfer from a photoexcited peptide to the solvent, *J. Chem. Phys.*, 2009, **131**, 184503.
44 P. H. Nguyen, S. Y. Park and G. Stock, Nonequilibrium molecular dynamics simulation of the energy transport through a peptide helix, *J. Chem. Phys.*, 2010, **132**, 025102.
45 J. D. Hartgerink, J. R. Granja, R. A. Milligan and M. R. Ghadiri, Self-assembly peptide nanotubes, *J. Am. Chem. Soc.*, 1996, **118**, 43–50.

